Journal of the Korean Physical Society, Vol. 46, No. 2, February 2005, pp. 482∼486

Optical Properties of $Ga_{1-x}Mn_xAs$ ($0 \leq x \leq 0.09$) Studied Using Spectroscopic Ellipsometry

Tae Dong KANG, Ghil Soo LEE and Hosun LEE*
Department of Physics, Kyung Hee University, Suwon 449-701

Dongwan KOH and Young Ju PARK
Nano-Device Research Center, Korea Institute of Science and Technology, Seoul 130-650

(Received 30 June 2004)

We investigate the optical properties of a series of $Ga_{1-x}Mn_xAs$ thin films by using spectroscopic ellipsometry. The $Ga_{1-x}Mn_xAs$ films are grown directly on GaAs (100) substrates by using molecular beam epitaxy. Using spectroscopic ellipsometry, we measure the pseudo-dielectric function for each of the films in the energy range between 1.0 – 6.0 eV. By using the Adachi lineshape model, we determined the dielectric functions and critical point parameters for the $Ga_{1-x}Mn_xAs$ films. We discuss the energy shifts associated with the E_1, $E_1 + \Delta_1$, E_0', and E_2 band gaps. We also discuss the band gap energy shift of $Ga_{1-x}Mn_xAs$ alloys as Mn is incorporated into the lattice.

PACS numbers: 71.20.Nr, 78.20.Ci, 78.66.Fd, 78.40.Fy
Keywords: GaMnAs, Ellipsometry, Band gap energy, Diluted magnetic system

I. INTRODUCTION

The prospect of using electron spins in electronic devices has generated much interest in diluted magnetic semiconductors (DMS). The discovery of ferromagnetism in III-V-based DMS up to 110 K, *e.g.*, $Ga_{1-x}Mn_xAs$ (abbreviated as GaMnAs hereafter), increased the possibility of realizing room-temperature ferromagnetic DMS. The ferromagnetism in p-type GaMnAs is known to be governed by the hybridization of Mn^{2+} d-state electrons with mobile holes and localized states near the top of the valence band [1]. Low-temperature epitaxial growth techniques have allowed the incorporation of Mn atoms beyond the equilibrium solubility limit [2]. In GaMnAs, the Mn composition can reach up to 9 atomic percent. The Mn atoms generally substitute at the Ga sites, forming a local magnetic moment, and act as acceptors, providing holes in the system. Ferromagnetic order is explained in terms of itinerent doped holes mediating the ferromagnetism of localized Mn spins.

Experimental methods have been used to understand the electronic band structure of GaMnAs such as photoemission spectroscopy and scanning tunneling microscopy [3,4]. However, optical studies have been very few. Singley *et al.* used infrared spectroscopy and observed a broad absorption resonance 0.2 eV above the valence band edge [5]. Ando *et al.* observed strong enhancement of magnetic circular dichroism from ferromagnetic GaMnAs and attributed it to a strong sp-d hybridization [6]. Seong *et al.* performed Raman spectroscopy and estimated the free hole concentration without the complexity of the anomalous Hall effect [7].

Several lineshape models, such as the standard critical point model, Fourier analysis, and the Holden model have been developed for determining the critical-point parameters [8–10]. Particularly, the analytical Adachi model can fit the dielectric function as well as the critical point parameters [11], and one can use a Gaussian-broadened Adachi model to improve the lineshape fitting [12].

In this work, we measured the pseudo-dielectric functions of GaMnAs ($0 \leq x \leq 0.09$) at room temperature in the spectral range between 1.0 eV and 6.0 eV. We used an Adachi-model dielectric function as the lineshape model in order to obtain the Mn composition dependence of the band gap energy. With increasing Mn composition, we found a small decrease in the E_1, E_0', and E_2 band gap energy as well as a constant $E_1 + \Delta_1$ band gap energies. We discuss the result in terms of the sp-d exchange effect.

II. EXPERIMENTS

The GaMnAs films were grown by usning a solid-source MBE system equipped with conventional Ga and Mn effusion cells and an As-cracker cell. The system

*E-mail: hlee@khu.ac.kr;
Present address: Department of Electrical Engineering, Virginia Commonwealth University, 601 W. Main St., Richmond, VA 23284-3072, USA

was equipped with a conventional RHEED (reflection of high energy electron diffraction) system for observing the *in-situ* epitaxial growth process and with a BandiT^{TM} temperature detector for measuring the real substrate temperature. The layer structures used in this work were in the following sequence: a GaAs buffer layer, a low-temperature (LT) GaAs buffer layer, and a GaMnAs layer with Mn concentrations of $0 \sim 0.09$. All samples were grown on (001) semi-insulating GaAs substrates under As-rich conditions by employing a beam flux with excess As. The GaMnAs layers were grown with various V/III flux ratios and Mn contents. A 300 nm-thick GaAs buffer layer was grown at 570 °C after the GaAs substrate deoxidation process. Subsequently, the substrate temperature, T_S, was lowered to 260 °C, and a 300 nm-thick GaAs layer was grown followed by a 750 nm-thick GaMnAs layer. We used the RHEED patterns to observe the changes in the surface reconstruction: First the GaAs buffer layer showed a (2×4) pattern, which changed to a $c(4 \times 4)$ pattern while T_S was being lowered to 260 °C. After the growth of LT GaAs buffer layer at 250 °C, the $c(4 \times 4)$ pattern changed abruptly into a (1×1) pattern, which was, in turn, changed into a (1×2) pattern during the growth of the GaMnAs layer [13]. We also investigated GaMnAs films ($x = 0.03, 0.05$) with a smaller thickness (75 nm), which showed higher ferromagnetic transition temperatures up to 65 K. The Mn compositions were estimated using X-ray diffraction and secondary ion mass spectroscopy [14].

We measured the pseudo-dielectric function of as-grown $Ga_{1-x}Mn_xAs$ ($0 \leq x \leq 0.09$) DMS by using spectroscopic ellipsometry. Spectroscopic ellipsometry measurements were performed on samples with incidence angles of 70° and 75° by using a variable angle ellipsometer [Woollam VASE model] with and without an auto-retarder in the spectral range of $1.0 \sim 6.0$ eV. The capability for multiple angles of incidence increased the accuracy in determining the dielectric function of the GaMnAs layer from the pseudo-dielectric functions. The pseudo-dielectric functions were fitted using a non-linear Levenberg-Marquardt algorithm with WVASE32 software. In addition, we tried to perform in-situ chemical etching to remove oxides with NH_4OH, which was diluted with methanol. The mixing ratio was 1 : 14. However, it did not improve the values of the pseudo-dielectric function.

III. RESULTS AND DISCUSSION

Figure 1 plots (a) the real and (b) the imaginary parts of the pseudo-dielectric functions of $Ga_{1-x}Mn_xAs$ ($0 \leq x \leq 0.09$), which were measured using spectroscopic ellipsometry between 1.0 eV and 6.0 eV at room temperature. Compared to the pseudo-dielectric functions of GaFeAs, the amplitude and the broadening of the pseudodielectric functions for GaMnAs did not decrease much, suggesting that the crystallinity of GaMnAs did not deteriorate much with increasing Mn composition [15]. Figure 2 plots the pseudo-dielectric functions of $Ga_{1-x}Mn_xAs$ for $x = 0$ and 0.07 and their curve fittings using Gaussian-broadened Adachi model. The fitting was excellent.

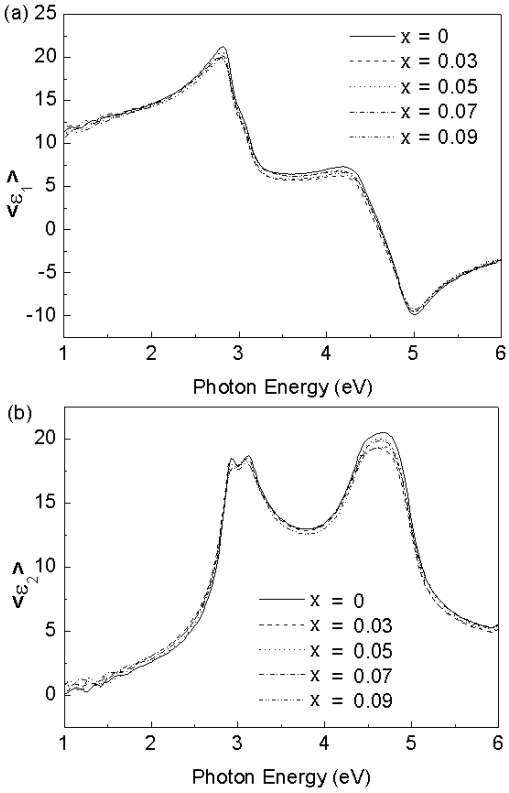

Fig. 1. Plots of (a) the real and (b) the imaginary parts of the pseudo-dielectric functions of $Ga_{1-x}Mn_xAs$ ($0 \leq x \leq 0.09$).

Adachi proposed an interband transition model for the dielectric function [10]. Assuming an energy-independent dipole matrix element, one can express the Adachi model dielectric function (MDF) for E_1 and $E_1 + \Delta_1$ as

$$\varepsilon(\omega) = -B_1\chi_1^{-2}ln(1-\chi_1^2) - B_{1s}\chi_{1s}^{-2}ln(1-\chi_{1s}^2), \quad (1)$$

with

$$\chi_1 = \frac{\hbar\omega + i\Gamma_1}{E_1}, \quad (2)$$

$$\chi_{1s} = \frac{\hbar\omega + i\Gamma_1}{E_1 + \Delta_1}. \quad (3)$$

Where B_1 (B_{1s}) is the strength of the E_1 ($E_1 + \Delta_1$). The exciton effect for E_1 and $E_1 + \Delta_1$ can be expressed as a Lorentzian lineshape in the form

$$\varepsilon(\omega) = \sum_{n=1}^{\infty}\left(\frac{B_{1x}}{E_1 - \hbar\omega - i\Gamma_1} + \frac{B_{2x}}{E_1 + \Delta_1 - \hbar\omega - i\Gamma_1}\right), \quad (4)$$

where B_{1x} (B_{2x}) is the strength of the E_1 ($E_1 + \Delta_1$)

exciton. The E_0' and E_2 transitions can be modeled using damped harmonic oscillators (j=1,2) with energy $E_{h,j}$:

$$\varepsilon(\omega) = \varepsilon_\infty + \sum_{j=1}^{2} \frac{C_{Ej} E_{h,j}^2}{E_{h,j}^2 - (\eta\omega)^2 - i\hbar\omega\Gamma_{Ehj}}. \quad (5)$$

The MDF for E_0 and $E_0 + \Delta_0$ is also given by the Adachi MDF model as follows:

$$\varepsilon(\omega) = A E_0^{-3/2} \left[f(\chi_0) + \frac{1}{2} \left(\frac{E_0}{E_0 + \Delta_0} \right)^{3/2} f(\chi_{s.o.}) \right] (6)$$

where

$$f(y) = y^{-2} \left[2 - (1+y)^{1/2} - (1-y)^{1/2} \right], \quad (7)$$

$$\chi = \frac{\hbar\omega + i\Gamma_0}{E_0}, \quad (8)$$

$$\chi_{s.o.} = \frac{\hbar\omega + i\Gamma_0}{E_0 + \Delta_0}, \quad (9)$$

where A and Γ_0 are the amplitude and the broadening parameters of the E_0 and the $E_0 + \Delta_0$ transitions, respectively.

We improved the lineshape fitting to $< \varepsilon >$ by replacing the damping constant Γ with a frequency-dependent

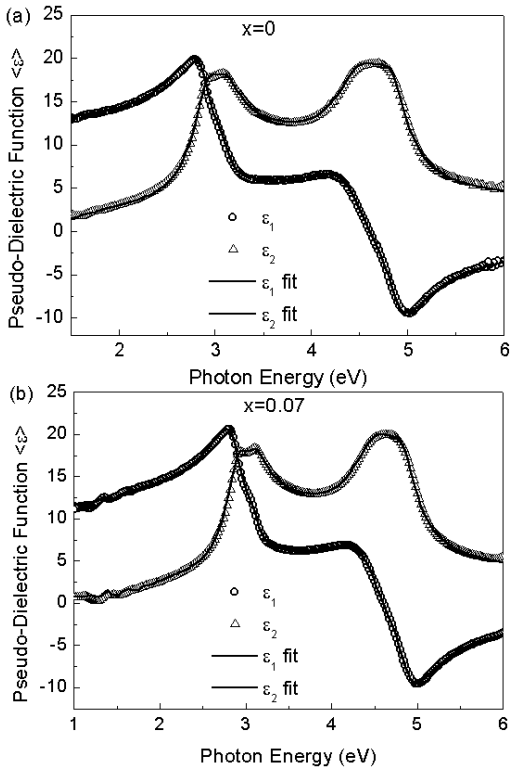

Fig. 2. Plots of the pseudo-dielectric functions of $Ga_{1-x}Mn_xAs$ for (a) $x = 0$ and (b) $x = 0.07$, and their curves fitted using the Gaussian-broadened Adachi MDF model.

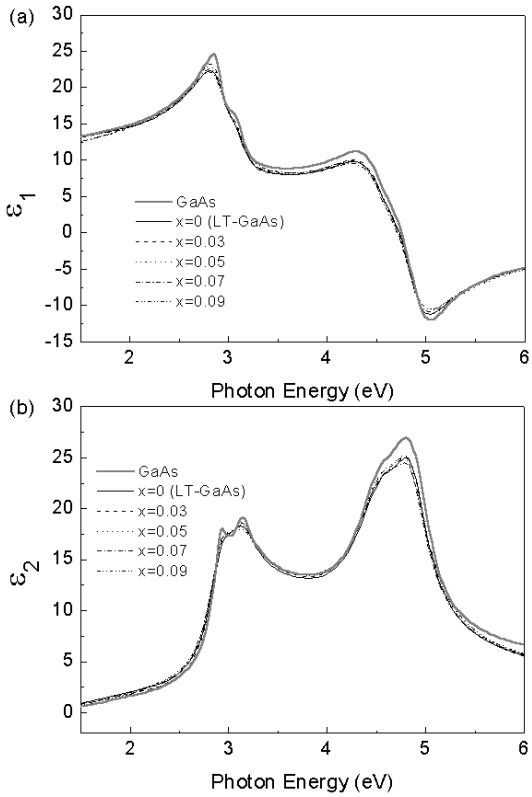

Fig. 3. (a) The real and (b) the imaginary parts of the fitted dielectric functions of GaMnAs from Fig. 1 by using the Gaussian-broadened Adachi MDF model assuming a GaAs oxide layer.

damping constant Γ' given by

$$\Gamma' = \Gamma \exp\left[-\alpha \left(\frac{\hbar\omega - \tilde{E}}{\Gamma} \right)^2 \right], \quad (10)$$

where $\tilde{E}$ is an appropriate threshold energy [12]. Note that we fixed the E_0 and the $E_0 + \Delta_0$ critical point parameter values. The fitted E_0 CP parameters have very large uncertainties because of their very small amplitudes and the overlapping with the E_1 gap.

Figure 3 is the fitted dielectric function of GaMnAs from Fig. 1 by using the Adachi MDF model and assuming a natural GaAs oxide layer. The GaAs oxide layer thicknesses were fitted to be about 2 nm. We do not see much change in the dielectric function of GaMnAs with increasing Mn composition.

Figure 4 is a plot of the fitted energies for E_1, $E_1 + \Delta_1$, E_0', and E_2 as functions of the Mn composition. The E_0 and $E_0 + \Delta_0$ band gap energy values were fixed as 1.41 and 1.74 eV. The E_1 energy decreased with increasing Mn composition whereas the $E_1 + \Delta_1$ energy did not change. The E_1 and $E_1 + \Delta_1$ transitions take place near the L point along the Λ directions of the Brillouin zone (BZ), where the valence bands and the conductions bands are nearly parallel. The E_0' transition, like the E_0

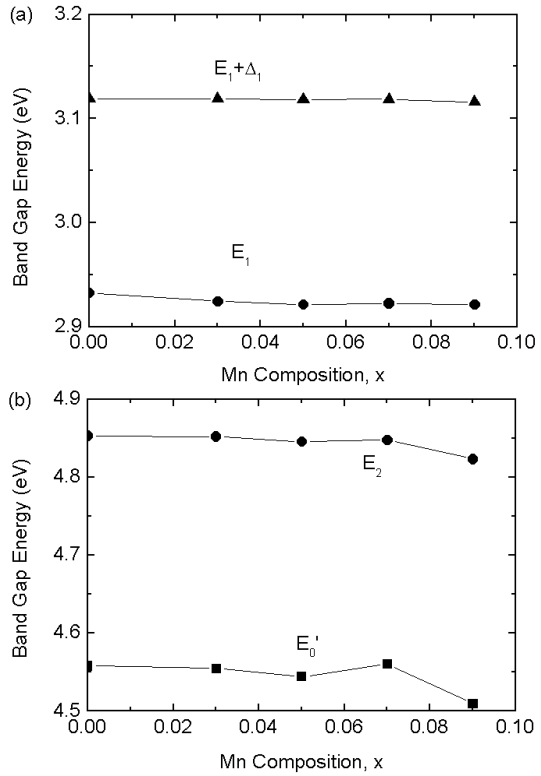

Fig. 4. Plots of the fitted band gap energies for (a) E_1 and $E_1 + \Delta_1$, and (b) E_0' and E_2 as functions of the Mn composition.

transition, occurs at or near the zone center, and it is the second lowest transition. The E_0 transition is the lowest transition and takes place at or near $k = 0$. The E_2 peak is actually composed of several peaks from mainly the $\sum$ line and the X point. The E_0' and the E_2 peak energies decrease with increasing Mn composition.

There are two models that can explain the band gap shift of E_1 and $E_1 + \Delta_1$. The first is the sp-d exchange model, which is based on the interaction between conduction electrons and localized magnetic impurity spins. The second is the sp-d hybridization model, which is based on the interaction of impurity d-levels and conduction electrons. In the case of transition-metal (Mn, Fe, Co)-doped ZnSe, the shift of the E_1 and the $E_1 + \Delta_1$ band gap energies due to the addition of transition-metal ions can be well explained by the sp-d hybridization model rather than the sp-d exchange model [16]. For example, the E_1 gap energy for ZnFeSe (ZnMnSe) increased (decreased) due to the repulsive interaction between the d levels of the transition metal ions and the L band of the host ZnSe. In the case of GaMnAs, the decrease in the E_1 energy with increasing Mn composition cannot be explained by using the sp-d hybridization of the d-level of Mn atoms and the GaAs L band. It predicts an increase in the E_1 gap because the Mn d-levels are below the GaAs L conduction band, so band repulsion will increase the E_1 band gap [17]. However, the sp-d exchange interaction predicts a decrease in E_1. Therefore, the sp-d exchange interaction may be the dominant mechanism rather than the sp-d hybridization interaction for the composition dependence of the E_1 gap in GaMnAs. The very small shift in the E_1 and the $E_1 + \Delta_1$ energies suggests that the substitution for Ga by Mn is incomplete, suggesting that some Mn ions are interstitial. We note that we investigated GaMnAs with varying critical temperatures. The CP energy values were independent of the critical temperatures.

IV. CONCLUSION

We measured the pseudo-dielectric functions of a series of $Ga_{1-x}Mn_xAs$ thin films by using spectroscopic ellipsometry. The $Ga_{1-x}Mn_xAs$ films were grown directly on GaAs (100) substrates by using molecular beam epitaxy at 260 °C. With the Adachi lineshape model and Gaussian-broadening, the dielectric functions for the $Ga_{1-x}Mn_xAs$ films were determined, taking into account of the oxide layer. The E_1, E_0', and E_2 band gap energies were observed to decrease whereas the $E_1 + \Delta_1$ band gap energy was constant. We explained the red shift of the E_1 band gap energy in terms of sp-d exchange model.

ACKNOWLEDGMENTS

This work was supported by a Korea Research Foundation grant No. KRF-2003-005-C00001.

REFERENCES

[1] P. M. Krstajić, V. A. Ivanov, F. M. Peeters, V. Fleurov and K. Kikoin, Europhys. Lett. **61**, 235 (2003), and references therein.
[2] H. Munekata, H. Ohno, S. von Molnar, A. Harwit, A. Segmüller and L. L. Chang, J. Vac. Sci. Tech. B **8**, 176 (1990).
[3] H. Åsklund, L. Ilver, J. Kanski, J. Sadowski and R. Mathieu, Phys. Rev. B **66**, 115319 (2002).
[4] T. Tsuruoka, N. Tachikawa, S. Ushioda, F. Matsukura, K. Takamura and H. Ohno, Appl. Phys. Lett. **81**, 2800 (2002).
[5] E. J. Singley, K. S. Burch, R. Kawakami, J. Stephens, D. D. Awschalom and D. N. Basov, Phys. Rev. B **68**, 165204 (2003).
[6] K. Ando, T. Hayashi, M. Tanaka and A. Twardowski, J. Appl. Phys. **83**, 6548 (1998).
[7] M. J. Seong, S. H. Chun, H. M. Cheong, N. Samarth and A. Mascarenhas, Phys. Rev. B **66**, 033202 (2002).
[8] M. Cardona, *Solid State Physics Suppl. 11*, edited by F. Seitz *et al.* (Academic Press, New York, 1969).
[9] D. E. Aspnes, Surf. Sci. **135**, 284 (1984).
[10] T. Holden, P. Ram, F. H. Pollak, J. L. Freeouf, B. X. Yang and M. C. Tamargo, Phys. Rev. B **56**, 4037 (1997).

[11] S. Ozaki and S. Adachi, J. Appl. Phys. **78**, 3380 (1995).
[12] A. D. Rakić and M. L. Majewski, J. Appl. Phys. **80**, 5909 (1996).
[13] D. Koh, K. S. Chung, J. B. Park, K. M. Kim, Y. J. Park, I. K. Han, J. I. Lee, Y. M. Kim and I.-W. Park, J. Korean Phys. Soc. **45**, 720 (2004).
[14] Y. J. Yoon, S. J. Chung, J. B. Park, H. J. Lee, S. Lee, S. Y. An, X. Liu and J. K. Furdyna, J. Korean Phys. Soc. **45**, 465 (2004).
[15] Hosun Lee, T. D. Kang, Y. J. Park, H. T. Oh, H. Y. Cho, R. Moriya and H. Munekata, J. Korean Phys. Soc. **42**, 441 (2003).
[16] Y. D. Kim, S. L. Cooper, M. V. Klein and B. T. Jonker, Phys. Rev. B **49**, 1732 (1994).
[17] P. Mahadevan and A. Zunger, Phys. Rev. B **69**, 115211 (2004).